

# Mobility of BtuB and OmpF in the *Escherichia coli* Outer Membrane: Implications for Dynamic Formation of a Translocon Complex

Jeff Spector,<sup>†</sup> Stanislav Zakharov,<sup>‡§</sup> Yoriko Lill,<sup>†</sup> Onkar Sharma,<sup>‡</sup> William A. Cramer,<sup>‡</sup> and Ken Ritchie<sup>†\*</sup>

<sup>†</sup>Department of Physics and <sup>‡</sup>Department of Biological Sciences, Purdue University, West Lafayette, Indiana; and <sup>§</sup>Institute of Basic Problems of Biology, Russian Academy of Sciences, Puschino, Moscow Region 140290, Russian Federation

**ABSTRACT** Diffusion of two *Escherichia coli* outer membrane proteins—the cobalamin (vitamin B12) receptor (BtuB) and the OmpF porin, which are implicated in the cellular import pathways of colicins and phages—was measured in vivo. The lateral mobility of these proteins is relevant to the mechanism of formation of the translocon for cellular import of colicins such as the rRNase colicin E3. The diffusion coefficient ( $D$ ) of BtuB, the primary colicin receptor, complexed to fluorescent antibody or colicin, is  $0.05 \pm 0.01 \mu\text{m}^2/\text{s}$  and  $0.10 \pm 0.02 \mu\text{m}^2/\text{s}$ , respectively, over a timescale of 25–150 ms. Mutagenesis of the BtuB TonB box, which eliminates or significantly weakens the interaction between BtuB and the TonB energy-transducing protein that is anchored in the cytoplasmic membrane, resulted in a fivefold larger value of  $D$ ,  $0.27 \pm 0.06 \mu\text{m}^2/\text{s}$  for antibody-labeled BtuB, indicating a cytoskeletal-like interaction of TonB with BtuB. OmpF has a diffusion coefficient of  $0.006 \pm 0.002 \mu\text{m}^2/\text{s}$ , ~10-fold smaller than that of BtuB, and is restricted within a domain of diameter 100 nm, showing it to be relatively immobile compared to BtuB. Thus, formation of the outer membrane translocon for cellular import of the nuclease colicins is a demonstrably dynamic process, because it depends on lateral diffusion of BtuB and collisional interaction with relatively immobile OmpF.

## INTRODUCTION

Phage and colicins parasitize outer membrane receptor proteins to generate a receptor-mediated pathway for their cellular import (1–3). The cobalamin receptor, BtuB, is required for the active transport of vitamin B12 (cobalamin) (4), as is the TonB protein that is anchored in the cytoplasmic membrane. TonB spans the periplasmic space and binds the TonB box in the N-terminus of BtuB, allowing TonB to transduce energy to the outer membrane that is supplied by the proton electrochemical potential gradient across the cytoplasmic membrane (5,6). The nuclease colicins, including colicin E3, which is the subject of this study and which exerts its cytotoxic effect in the cytoplasm as an rRNase, use BtuB (7–9) for initial docking to the extracellular surface of the *Escherichia coli* outer membrane. BtuB, present at a copy number of 200–400 molecules/cell (4), serves as the primary outer membrane receptor for at least seven colicins whose cytotoxicity is expressed through pore formation in the cytoplasmic membrane or as intracellular nucleases (10). The crystal structure of the 22-stranded  $\beta$ -barrel BtuB in the absence of colicin has been solved to high resolution in a detergent matrix (11), and in the lipidic cubic phase to 1.95 Å (12). Crystal structures of BtuB, in a complex with the receptor binding domain of colicin E3 (8) or colicin E2 (13) have also been solved.

These nuclease colicins also utilize the aqueous transmembrane channels of the trimeric 16-stranded  $\beta$ -barrel outer membrane protein (Omp)F (14–18) or OmpC (2,19) porin, present at a level of  $\sim 10^5$  copies/cell,  $\sim 1000$  times greater than the content of BtuB (20), for the entry pathway of the colicin C-terminal catalytic domain through the outer membrane. Several lines of evidence, including crystal structures of BtuB complexed to the receptor binding domain of the nuclease colicins (8,13), a crystal structure of OmpF with the disordered N-terminal peptide of colicin E3 bound in its lumen (17), binding of OmpF to a complex of BtuB and the nuclease colicin E9 (15), and occlusion of OmpF channels by colicin E3 and T- and C-domain peptides (16,18), have led to a model for an outer membrane translocon for nuclease colicins that consists of a complex of BtuB and OmpF (8,17), formed at least transiently. However, there is no experimental precedent for a preformed complex of the two outer membrane proteins, BtuB and OmpF. Therefore, it is proposed that formation of the BtuB/OmpF/colicin E3 translocon in the outer membrane requires efficient lateral diffusion of BtuB and/or OmpF in the outer membrane to form a transient complex that is used for colicin import.

A study of the lateral diffusion of outer membrane proteins in Gram-negative bacteria is of particular interest because of the unique bipartite structure of this membrane in which the inner and outer leaflets of this membrane consist of phospholipid and lipopolysaccharide (3), respectively, and a hydrophobic width that appears to be significantly smaller than the typical lipid bilayer (12).

Two previous studies using the technique of single particle tracking have investigated the mobility of the outer

Submitted May 27, 2010, and accepted for publication October 7, 2010.

\*Correspondence: [kpitchie@purdue.edu](mailto:kpitchie@purdue.edu)

Jeff Spector's present address is National Institute of Standards and Technology, Gaithersburg, MD 20899.

Onkar Sharma's present address is Department of Microbiology and Molecular Genetics, Harvard Medical School, Boston, MA 02115.

Editor: George Barisas.

© 2010 by the Biophysical Society  
0006-3495/10/12/3880/7 \$2.00

doi: [10.1016/j.bpj.2010.10.029](https://doi.org/10.1016/j.bpj.2010.10.029)

membrane protein  $\lambda$ -receptor (LamB), the maltodextrin transport channel in *E. coli*, with somewhat different results. Oddershede et al. (21) measured the local diffusion coefficient of LamB by attaching a 530-nm microsphere and imaging the microspheres at 25 Hz. Measurements were performed using weak laser optical tweezers to hold the microsphere/ $\lambda$ -receptor complex. The local short-time diffusion coefficient for the  $\lambda$ -receptor was  $0.15 \pm 0.10 \mu\text{m}^2/\text{s}$ . In the absence of the laser tweezers, long-range diffusion was not observed and LamB was found to be confined within a domain of diameter 29 nm. Gibbs et al. (22) employed 20-nm diameter gold as labels for LamB imaged at 1 Hz. They classified the mobility of LamB into a slow (~60%) and fast moving population (~40%). The slowly moving population remained in a 20–50 nm compartment over the 5-min observation. This compartmentalization is consistent with the results of Oddershede et al. (21). The faster moving population was found to traverse 100–300 nm in the 5-min observation window. Although not stated in Gibbs et al. (22), this would imply a very small diffusion coefficient of  $\sim 10^{-4}$ – $10^{-5} \mu\text{m}^2/\text{s}$  for the fast component over long times.

To probe the mobility of the major components of the BtuB-colicin E3-OmpF translocon complex, single molecule imaging was performed on BtuB or OmpF in the outer membrane of viable *E. coli* cells. BtuB or OmpF were complexed to a ligand or antibody containing a fluorescent tag:

1. BtuB receptor and Alexa Fluor-555-tagged anti-BtuB antibody.
2. BtuB receptor and Oregon Green 488 tagged colicin E3.
3. A mutant of BtuB with reduced interaction to TonB and Alexa Fluor 555 tagged anti-BtuB antibody.
4. The OmpF porin and Alexa Fluor 555 tagged anti-OmpF antibody.

## MATERIALS AND METHODS

### Labeling of BtuB, colicin E3, and OmpF

Diffusion of wild-type BtuB was measured in the outer membrane of viable *E. coli* strain K17; BtuB with a mutated TonB box (BtuB Asp<sup>6</sup>Ala-Thr<sup>7</sup>Ala-Leu<sup>8</sup>Ala-Val<sup>9</sup>Ala) was cloned in a pET41b vector and subsequently expressed in the  $\Delta\text{btuB}$  strain. Diffusion was observed through labeling of BtuB with antibody or colicin E3 to which a fluorophore was bound. OmpF porin diffusion was observed through fluorophore-labeled anti-OmpF polyclonal antibody. Anti-BtuB or anti-OmpF polyclonal antibody was labeled with Alexa Fluor 555 using the antibody-labeling protocol and reagents from Invitrogen/Molecular Probes (Eugene, OR). A Lys<sup>549</sup>Cys mutant of colicin E3 was labeled with Oregon Green 488 using its 6-iodoacetamide derivative (i.e., mixed isomers; Invitrogen/Molecular Probes), as described elsewhere (23).

### Sample mounting

Glass-bottom cover dishes were used as sample chambers. The cover dishes were cleaned in 5% Contrad detergent (Decon, King of Prussia, PA) over-

night, sonicated 30 min, immersed in 0.1 M KOH overnight, sonicated 30 min, and rinsed. Before use, 100  $\mu\text{L}$  of 0.1 mg/mL poly-L-lysine (MW 70,000–150,000; Sigma-Aldrich, St. Louis, MO) was adsorbed to the cover glass. Excess poly-L-lysine solution was removed and the cover glass was washed. A suspension of *E. coli* was placed in the chamber and allowed to adhere to the poly-L-lysine layer for 20 min in minimal media. Excess nonadherent cells were washed away in phosphate-buffered saline (pH 7.4) and  $\sim 1$  fM, final concentration, of antibody or colicin E3 was added to the chamber before observation.

### Oblique angle epifluorescence imaging

Imaging was performed using oblique-angle laser illuminated epifluorescence microscopy where an argon-ion (488 nm) or He-Ne (543 nm) (Spectra Physics, Newport, Irvine, CA) laser was used, respectively, to excite labeled colicin or antibody (Fig. 1). The fluorescence emission was defined, respectively, by 500–550 nm and 562.5–637.5-nm band-pass filters (Chroma Technology, Bellows Falls, VT). The laser beam was directed by a dichroic mirror (Chroma Technology) off the optical axis through the objective (1.45 NA oil immersion, Olympus America, Melville, NY) so as to illuminate only the adherent cells and not the entire sample chamber. Fluorescence emission was collected through the dichroic mirror and an emission filter on a dual multichannel-plate intensified Peltier-cooled charge-coupled device camera (Turbo-120Z; Stanford Photonics, Palo Alto, CA) at 40 Hz. Image magnification was such that the pixel resolution was 70 nm/pixel at the camera.

### Single molecule tracking and mobility analysis

The apparent position of the labeled molecule in the video image was determined as described by Gelles et al. (24). A kernel was developed from a Gaussian distribution which was then cross-correlated with each subsequent video frame in the neighborhood of the last position of the label of interest. For each frame, the center of geometry of the portion of the

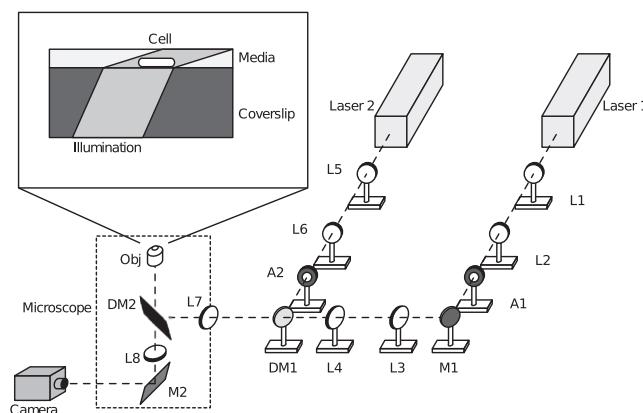


**FIGURE 1** Oblique-angle laser illuminated epifluorescence microscopy schematic: The illumination pathway consists of two lasers (*Laser 1*, 2 mW He-Ne 543 nm; *Laser 2*, 100 mW Argon Ion 488 nm), 10 $\times$  beam expander optics (*L1*, *L2*; *L5*, *L6*), field stop (*A1*, *A2*), and steering mirrors (100% mirror *M1*; Laser combiner dichroic mirror, *DM1*). Lens *L3* and *L4* are used to project *M1* onto *DM1*. Within the microscope, lens *L7* couples the center of *DM1* and *M1* to the focal plane through dichroic mirror *DM2* and an Olympus 100 $\times$  1.4 NA oil immersion lens. The image of the emission from the sample is projected by lens *L8* through mirror *M2* to a dual multichannel plate intensified, cooled charge-coupled device camera (Model XR/Turbo-120Z; Stanford Photonics). An expanded view of the oblique illumination of the sample is shown.

correlation intensity above a chosen threshold value was used to locate the molecules position.

Quantitative analysis of the mobility was carried out by first calculating the mean-square displacement (MSD),  $\langle r^2(t) \rangle$ , of the observed label for each trajectory according to (25,26)

$$\langle r^2(n \delta t) \rangle = (N - 1 - n)^{-1} \sum_{j=1}^{N-1-n} [x(j \delta t + n \delta t) - x(j \delta t)]^2 + [y(j \delta t + n \delta t) - y(j \delta t)]^2,$$

where  $\delta t$  is the time resolution and  $x(j \delta t + n \delta t)$ ,  $y(j \delta t + n \delta t)$  describes the particle position after a time interval  $n \delta t$  after starting at position  $x(j \delta t)$ ,  $y(j \delta t)$ ,  $N$  is the total number of frames in the sequence, and  $n$  and  $j$  are positive integers.

The average MSD at each time delay for a given set of experiments was determined by averaging over the MSD calculated for each trajectory for which the fluorophore could be imaged for at least 10 frames (250 ms). Assuming random Brownian motion, the MSD should increase linearly in time as  $\langle r^2(t) \rangle = 4Dt + \delta^2$ . The effective diffusion coefficient,  $D$ , was determined by a linear fit to the average MSD over the first six delay times (25–150 ms) (27). The y-intercept,  $\delta^2$ , is due to the finite accuracy with which the particle position can be measured and is independent of the time delay between measurements. As such,  $\delta^2$  enters as a constant added to the MSD at all time delays and can be removed by estimating the y-intercept of the MSD-versus-time-delay-plot at short times. The first six time delays, 25–150 ms, were used in this estimate. Note that the addition of this error term does not affect the estimate of the diffusion coefficient from the slope of MSD-versus-time-delay-plot because the error is time-independent.

Analysis assuming anomalous subdiffusive motion proceeded by fitting the plot of the entire average MSD versus time to 250 ms with the relation  $\langle r^2(t) \rangle = 4D^*t^\alpha + \delta^2$ , where the prefactor  $D^*$  is a transport coefficient with units of  $\text{length}^2/\text{time}^\alpha$  and the time exponent  $\alpha$  is expected to be unity for Brownian motion and less than unity for subdiffusive processes (28). The value  $\delta^2$  is the y-intercept of the data, which is related to the accuracy of the determination of the position of the fluorophore in each frame.

## Simulated diffusion on the *E. coli* surface

An idealized *E. coli* cell was constructed as a 1- $\mu\text{m}$  length, 500-nm radius cylinder capped by 500-nm radius hemispheres at each end. A Monte Carlo simulation (29) of the Brownian motion of a protein on this surface was performed by starting at a random position on the surface and taking successive equal arc-length steps in random directions for each time step. The position of the diffusant was recorded every 25,000 time steps (corresponding to an experimental frame rate of 40 fps; i.e., each step in the simulation corresponds to a microsecond increment in time). These positions were projected onto a two-dimensional plane to simulate the image recorded in an actual experiment. The size of the length step was set so that the analyzed two-dimensional diffusion coefficient for the simulation was comparable to the experimental value determined for BtuB labeled with colicin E3. A total of 100 runs of 20 frames each was performed. Analysis proceeded identically to that of the experimentally determined trajectories described above.

## RESULTS AND DISCUSSION

### Diffusion of antibody-labeled BtuB and OmpF

Trajectories of individual BtuB molecules were recorded after labeling with Alexa 555-anti-BtuB antibody using oblique-angle laser illuminated epifluorescence microscopy, as shown in Fig. 1 and described in Materials and Methods. Only trajectories of molecules bound by individual fluores-

cent labels chosen by observing single-step photobleaching of the label at the end of the observation were analyzed. The MSD for different time delays were determined from the observed trajectories of BtuB in the outer membrane of individual *E. coli* cells. The average MSD, determined by averaging over all trajectories for which the fluorophore could be imaged for at least 10 frames (250 ms), with BtuB complexed to labeled antibody, is shown (Fig. 2). The diffusion coefficient,  $D$ , was determined by the slope from a fitted linear regression to the MSD for the first six time delays (25–150 ms) (27). The diffusion coefficient of the complex of BtuB with labeled antibody was  $0.05 \pm 0.01 \mu\text{m}^2/\text{s}$  (number of trajectories analyzed,  $n = 101$ ).

The MSD, displayed as a function of the time delay, for OmpF labeled by Alexa 555-anti-OmpF is shown in Fig. 3. In comparison to the fast mobility of BtuB, OmpF is found to have a diffusion coefficient that is an order-of-magnitude smaller,  $0.006 \pm 0.002 \mu\text{m}^2/\text{s}$  ( $n = 172$ ). The diffusion of OmpF, although relatively slow, can be distinguished from that of fluorescent-labeled antibody to BtuB immobilized on a glass coverslip, which would measure any drift of the chamber during the time of the experiment (Fig. 3, open squares). As shown in Fig. 3, at times  $>0.15$  s, OmpF attains a maximum MSD of  $0.0035 \text{ nm}^2$  (after correction for the y-intercept at  $t = 0$  which removes the effects of localization error) or a maximum root-mean-square displacement of  $\sim 60$  nm. For diffusion within a domain of diameter,  $L$ , with hard impenetrable walls, it is known that the time dependence of MSD asymptotically approaches a value of  $\langle r^2 \rangle_t \rightarrow \infty \rightarrow L^2/3$  (25). This maximum displacement implies confinement of OmpF in a domain of diameter 100 nm within the outer membrane. It is expected that the confinement size is actually somewhat larger than measured due to the effects of averaging the position of the labeled OmpF during each exposure to the camera during observation (30). A more precise estimate of the domain size would require much higher frame-rate video imaging than employed in this study.

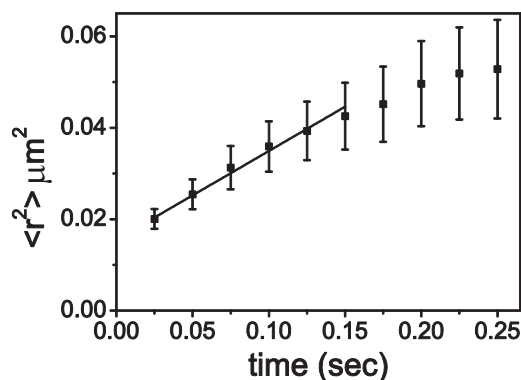


FIGURE 2 Determination of the diffusion coefficient of BtuB using fluorescent-labeled antibody. Time dependence of MSD of wild-type BtuB, complexed to labeled anti-BtuB. (Solid line) A fit to the MSD for the first six time delays (25–150 ms) was used to determine the diffusion coefficient.

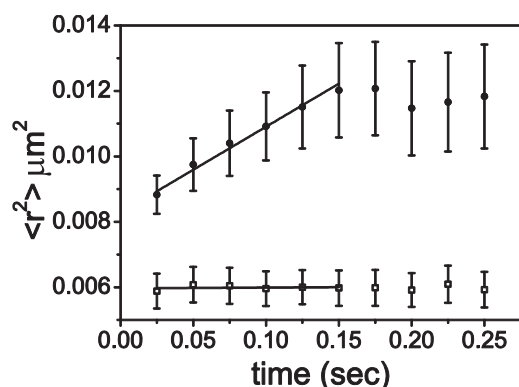


FIGURE 3 Determination of the relatively slow diffusion of OmpF. Mean-square displacement of anti-OmpF-labeled OmpF (solid circles) to anti-BtuB immobilized on glass (open squares) as a function of time. (Solid line) A fit to the MSD for the first six time delays (25–150 ms) was used to determine the diffusion coefficient.

In terms of long-range mobility, the average distance traversed by anti-BtuB labeled BtuB in 0.25 s would be 190 nm and hence BtuB displays a much increased long-range mobility in comparison with the 5-min timeframe required to travel 300 nm from the previous reports of the diffusion of LamB (22). In comparison, OmpF shows restricted motion within domains of size 100 nm, which is similar to the fraction of LamB for which restricted motion was reported, but displays a diffusion coefficient that is reduced  $\sim 25$ -fold from the value of  $0.15 \pm 0.10 \mu\text{m}^2/\text{s}$  for LamB within a domain of size 29 nm determined at comparable frame rates (21).

### Interaction of BtuB with TonB reduces mobility of BtuB

TonB, which is embedded in the cytoplasmic membrane and spans the periplasmic space, is required for signaling and cobalamin uptake through BtuB (5,6). TonB interacts with BtuB through a seven-residue peptide sequence, the TonB box, near the N-terminus of BtuB (the sequence in BtuB is DTLVVTA, residues 6–12) (12). To determine the effect of the BtuB-TonB interaction on the BtuB lateral mobility, a mutation was introduced into BtuB to eliminate or significantly impair the attachment of BtuB to TonB. Single residue mutations in this segment have been shown previously to result in a loss of transport, but do not affect the entry of the TonB-independent phage BF23 and E colicins (31,32).

Here, the TonB box was changed through a four-site mutation, Asp<sup>6</sup>Ala-Thr<sup>7</sup>Ala-Leu<sup>8</sup>Ala-Val<sup>9</sup>Ala. The value of the diffusion constant for the mutationally altered BtuB, determined from the time dependence of the MSD versus time, was  $0.27 \pm 0.06 \mu\text{m}^2/\text{s}$  ( $n = 71$ ), approximately fivefold larger than that of wild-type BtuB with attached labeled antibody (Fig. 4). The mutant BtuB protein,

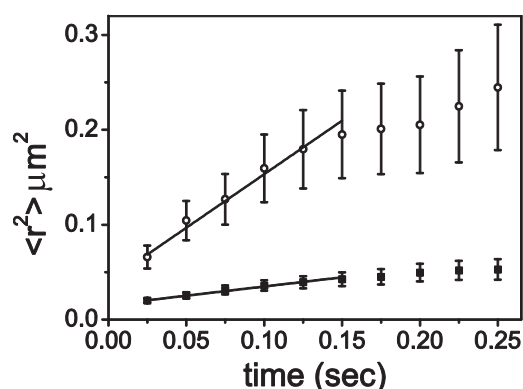


FIGURE 4 Lateral diffusion of BtuB is retarded by interaction with TonB. Time dependence of the MSD of wild-type BtuB complexed to labeled anti-BtuB (solid squares) and to labeled anti-BtuB antibody/mutant BtuB (open circles). (Solid line) Fits to the MSD for the first six time delays (25–150 ms) was used to determine the diffusion coefficients.

unfettered by the TonB protein, travels an average distance of 450 nm in 0.25 s. Thus, interactions between BtuB and TonB result in a significant reduction of the lateral mobility of BtuB and, in this respect, resemble the interaction of integral membrane proteins that are connected to cytoskeletal elements (33).

The fivefold increase in the diffusion coefficient of antibody-labeled BtuB upon the weakening of its interaction with TonB implies that these interactions are responsible, at least in part, for the slower average diffusion observed for wild-type BtuB. While TonB itself may be mobile in the cytoplasmic membrane, interaction between TonB and BtuB requires TonB to span the periplasmic space through the peptidoglycan layer. As such, we assume that during the times when BtuB is in direct contact with TonB, the complex is immobile in both membranes due to the influence of the peptidoglycan layer. Further, if we assume that the TonB box mutant of BtuB is completely free of interaction with TonB, then it is inferred:

1. The true (free of specific interaction) diffusion coefficient of BtuB is that of the mutant BtuB,  $0.27 \pm 0.06 \mu\text{m}^2/\text{s}$ .
2. The wild-type BtuB is stationary when interacting with TonB, and moves with a diffusion coefficient equal to that of the mutant when not interacting with TonB.
3. The fivefold reduction in the diffusion coefficient of wild-type BtuB is a consequence of BtuB interacting with TonB 80% of the time, which forms a lower bound due to the extreme assumption of immobility of the complex during interaction.
4. The interactions between TonB and BtuB occur on time-scales faster than 25 ms (the imaging timescale) because there was no direct evidence of the TonB-BtuB interaction (i.e., BtuB was not found to slow or temporarily stop during its trajectories, although such motion is hard to discern statistically from random motion in the short trajectories observed in these studies).



## Diffusion of colicin E3 bound to the *E. coli* outer membrane

Upon introduction of colicin E3 labeled with the fluorophore Oregon Green 488 into the sample medium, the colicin is observed to bind to the *E. coli* cells containing the BtuB receptor, and to diffuse in the membrane. The mobility of BtuB labeled with antibody (Fig. 5, *solid squares*) or labeled colicin E3 is compared. The diffusion coefficient of BtuB complexed to colicin E3, calculated to be  $0.10 \pm 0.02 \mu\text{m}^2/\text{s}$  ( $n = 70$ ), is approximately twofold larger than when complexed to the labeled antibody. Further colicin E3-labeled BtuB was also found not to slow or temporarily stop during its trajectories (although such motion is, again, hard to discern statistically from random motion in the short trajectories observed in these studies), implying that the colicin E3-BtuB complex does not bind to the slowly diffusing OmpF during observation.

The slightly increased value of the diffusion coefficient for BtuB tagged with colicin E3 compared to antibody-labeled BtuB suggests that the binding of colicin E3 to BtuB results in a weakened BtuB-TonB interaction, which could explain why the import and cytotoxicity of the colicin is TonB-independent. Consistent with this inference is a measurement of reduced accessibility of residues in the TonB box (34) associated with binding of the colicin E3 receptor binding (R)-domain to BtuB. On the other hand, at a resolution of 2.7 Å, the crystal structure of the complex of BtuB and the R-domain shows little conformational change in the TonB box region upon binding of the colicin E3 R-domain (8).

Two other possible explanations for the increase in diffusion coefficient of BtuB upon colicin E3-labeling compared to antibody-labeling are:

1. The colicin may exchange between BtuB molecules during observation; and

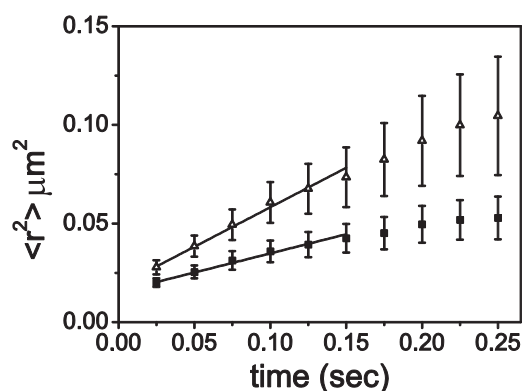


FIGURE 5 Comparison of diffusion of BtuB labeled with fluorescent antibody or colicin. Time dependence of MSD of wild-type BtuB complexed to labeled anti-BtuB (*solid squares*) and to labeled colicin E3 (*open triangles*). (*Solid line*) Fits to the MSD for the first six time delays (25–150 ms), used to determine diffusion coefficients.

2. The antibody may crosslink BtuB molecules and, hence, slow their diffusion compared to the monovalent labeling of the colicin E3.

Any exchange of the colicin involving release from BtuB is unlikely, because the  $K_d$  for the dissociation of colicin from BtuB is  $\leq 1\text{--}2 \text{ nM}$  (8,15). Thus, it is not expected the colicin E3 label dissociates from an individual BtuB during observation. Further, due to the sparse distribution of BtuB in the membrane (total copy number of  $\sim 200\text{--}400$  molecules/cell (4)) and because observation of the probes occurred as the probes first landed on the cell, we expect that, during observation, the antibody is most likely bound to a single BtuB molecule.

## Analysis of anomalous BtuB diffusion

From the MSD of BtuB (Fig. 2) and BtuB mutated in the TonB box (Fig. 4), it is apparent that the diffusion of BtuB in the outer membrane is not described by Brownian diffusion over the entire timescale. Its motion can be described as an anomalous subdiffusive process where the evolution of the MSD,  $\langle r^2 \rangle$ , as a function of time,  $t$ , is described by the proportionality,  $\langle r^2 \rangle \sim t^\alpha$ , where  $0 < \alpha < 1$ . Fig. 6 presents a fit to the data shown in Figs. 2 and 4 of the equation

$$\langle r^2 \rangle = D^* t^\alpha + \delta^2,$$

where the coefficient  $D^*$  is a modified diffusion coefficient with units of  $\text{length}^2/\text{time}^\alpha$  and  $\delta^2$  is the y-intercept of the data which arises from limitations in the precision of measurement. The best fit of  $\alpha$  over the entire timescale of the data (25–250 ms) for antibody-labeled wild-type BtuB, antibody-labeled mutant BtuB, and the adduct of BtuB and colicin E3 was  $0.56 \pm 0.06$ ,  $0.56 \pm 0.12$ , and  $0.75 \pm 0.05$ , respectively. For antibody-labeled OmpF, the best fit of  $\alpha$  over the 25–250 ms timescale was  $0.14 \pm 0.01$ .

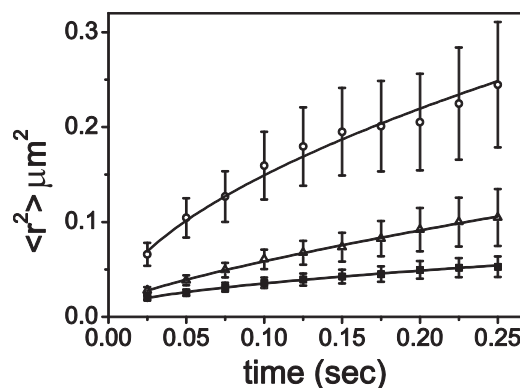


FIGURE 6 Analysis of anomalous BtuB diffusion. Time dependence of MSD for: (i) labeled anti-BtuB antibody/wild-type BtuB (*solid squares*), (ii) labeled colicin E3/wild-type BtuB (*open triangles*), and (iii) labeled anti-BtuB antibody/mutant BtuB (*open circles*). (*Solid line*) Fits to the MSD ( $\langle r^2 \rangle$ ) over all time for anomalous subdiffusion, utilizing the formula ( $\langle r^2 \rangle = D^* t^\alpha + \delta^2$ ).

## Diffusion on the curved *E. coli* surface: Monte Carlo simulations

To confirm that the anomalous diffusion did not arise from the curved geometry of the *E. coli* cell surface, simulations of Brownian motion on the surface of a cylinder with hemispherical caps were performed. Analysis of the simulated motion, projected on to a two-dimensional plane (as the motion is observed in the experiments) yields a value of  $\alpha = 0.995 \pm 0.004$ . Thus, it is apparent that the anomalous diffusion observed in the experiments is not a consequence of the curved geometry of the cell surface.

The qualitative effect of the anomalous subdiffusion is to decrease the value of the lateral diffusion coefficient measured at long times. This effect may be attributed to a high density of outer membrane proteins (20,35) that would restrict motion over long distances and times. Interestingly, OmpF displays both a small diffusion coefficient,  $0.006 \pm 0.002 \mu\text{m}^2/\text{s}$ , and a small anomalous exponent,  $\alpha = 0.14 \pm 0.01$ , when compared to BtuB which ranges from 0.05 to  $0.27 \mu\text{m}^2/\text{s}$  and 0.56–0.75, respectively. One might hypothesize that this implies that OmpF and BtuB reside in separate domains within the outer membrane, a crowded domain containing OmpF and a less crowded domain containing BtuB. A complete description of the surface density distribution of OmpF or of other proteins in the *E. coli* outer membrane does not presently exist, though a major Omp protein, presumably OmpF or OmpC, can form a paracrystalline array in the outer membrane (35). The conditions that generate such crystalline array are under study (W. A. Cramer and M. V. Zhahnina (Purdue University), unpublished). These studies, together with the data presented in this article, are first steps toward a map of OmpF density in the outer membrane and should lead to a deeper understanding of the mechanism behind the observed anomalous diffusion.

## Formation of the colicin translocon relies on BtuB diffusion and collisional interaction with OmpF porin

The events required to form the colicin translocon in the outer membrane, initiated by binding of the colicin to the BtuB primary receptor, thus transferring it to the two-dimensional space of the outer membrane surface, followed by diffusion, fishing for, and binding to, the OmpF receptor/translocator, are summarized in Fig. 7. The existence of a translocon for protein import/secretion that does not exist as a permanent complex in the membrane, but is formed by lateral diffusion and collisional interaction, is unprecedented. It is noted that a conceptually similar conclusion has been reached regarding dynamic formation of the flagellar motor (36). There is no indication that other membrane protein translocons for which there are existing crystal structures (37–39), are assembled through diffu-

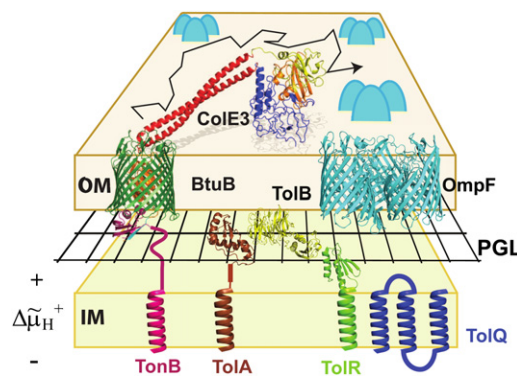


FIGURE 7 The outer membrane translocon for nuclease E colicins (multicolored molecule above the outer membrane) formed by diffusion of BtuB (dark green) and collisional interaction with OmpF (cyan). Cellular import of cytotoxic colicin E3 begins with translocation through the outer membrane (OM), which is initiated by tight binding ( $K_d < 10^{-9}$  M) of the apex of the 100 Å long coiled-coil domain to the parasitized vitamin B12 receptor, BtuB (8,13). Subsequently, lateral diffusion of BtuB (Figs. 2 and 4) enables binding of the T- and C-domains of the colicin to OmpF (16,18), allowing the C-domain to enter the cell through the OmpF pore, as demonstrated in the crystal structure of a complex of OmpF and a disordered N-terminal domain inserted into OmpF (17). The catalytic C-domain, in a disordered state (18), would pass through the outer membrane through a mechanism dependent upon binding of the N-terminal TolB box of the colicin to the periplasmic TolB protein (yellow) (44,45), concomitant proteolytic cleavage (34), and liberation of the C-domain. The TonB protein (magenta), required for active transport of vitamin B12, is bound to BtuB through its C-terminal periplasmic domain, impedes diffusion of BtuB (Fig. 6). The TolQ, R, and A components of the inner membrane translocon for the colicin C-domain are shown (blue, light green, and brown, respectively), as is the ultimate source of energy for colicin import, the proton electrochemical potential gradient,  $\Delta\mu_{H^+}$ , across the inner membrane (IM). Peptidoglycan layer (PGL).

sion/collision of component subunits. Import of colicin Ia may involve such an interaction between two molecules of its Cir outer membrane receptor (40). The subsequent import of the catalytic domain of the endo-ribonucleolytic C-domain of colicin E3 (41,42) and other nuclease colicins to the cytoplasm (43) also requires translocation through the inner membrane, utilizing a mechanism not yet elucidated, which utilizes the three subunit membrane-embedded TolQRA complex in the cytoplasmic membrane (10,44).

We thank M. V. Zhahnina for contributions to these experiments.

These studies were supported by grant No. 0646633 from the National Science Foundation (to K.R.), National Institutes of Health grant No. GM-18457 and the Henry Koffler Professorship (to W.A.C.).

## REFERENCES

1. Luria, S. E., and J. L. Suit. 1987. Colicins and col plasmids. In *Escherichia coli and Salmonella typhimurium: Cellular and Molecular Biology*. F. C. Neidhardt, editor. American Society of Microbiologists, Washington, DC. 1615–1624.
2. Mock, M., and A. P. Pugsley. 1982. The BtuB group col plasmids and homology between the colicins they encode. *J. Bacteriol.* 150:1069–1076.

3. Nikaido, H., and M. Vaara. 1987. Outer membrane. In *Escherichia coli* and *Salmonella typhimurium*: Cellular and Molecular Biology. F. C. Neidhardt, editor. American Society of Microbiologists, Washington, DC. 7–22.
4. Di Masi, D. R., J. C. White, ..., C. Bradbeer. 1973. Transport of vitamin B12 in *Escherichia coli*: common receptor sites for vitamin B12 and the E colicins on the outer membrane of the cell envelope. *J. Bacteriol.* 115:506–513.
5. Ollis, A. A., M. Manning, ..., K. Postle. 2009. Cytoplasmic membrane protonmotive force energizes periplasmic interactions between ExbD and TonB. *Mol. Microbiol.* 73:466–481.
6. Gumbart, J., M. C. Wiener, and E. Tajkhorshid. 2007. Mechanics of force propagation in TonB-dependent outer membrane transport. *Biophys. J.* 93:496–504.
7. Imajoh, S., Y. Ohno-Iwashita, and K. Imahori. 1982. The receptor for colicin E3. Isolation and some properties. *J. Biol. Chem.* 257:6481–6487.
8. Kurisu, G., S. D. Zakharov, ..., W. A. Cramer. 2003. The structure of BtuB with bound colicin E3 R-domain implies a translocon. *Nat. Struct. Biol.* 10:948–954.
9. Taylor, R., J. W. Burgner, ..., W. A. Cramer. 1998. Purification and characterization of monomeric *Escherichia coli* vitamin B12 receptor with high affinity for colicin E3. *J. Biol. Chem.* 273:31113–31118.
10. Cascales, E., S. K. Buchanan, ..., D. Cavard. 2007. Colicin biology. *Microbiol. Mol. Biol. Rev.* 71:158–229.
11. Chimento, D. P., A. K. Mohanty, ..., M. C. Wiener. 2003. Substrate-induced transmembrane signaling in the cobalamin transporter BtuB. *Nat. Struct. Biol.* 10:394–401.
12. Cherezov, V., E. Yamashita, ..., M. Caffrey. 2006. In meso structure of the cobalamin transporter, BtuB, at 1.95 Å resolution. *J. Mol. Biol.* 364:716–734.
13. Sharma, O., E. Yamashita, ..., W. A. Cramer. 2007. Structure of the complex of the colicin E2 R-domain and its BtuB receptor. The outer membrane colicin translocon. *J. Biol. Chem.* 282:23163–23170.
14. Bénédetti, H., M. Frenette, ..., C. Lazdunski. 1989. Comparison of the uptake systems for the entry of various BtuB group colicins into *Escherichia coli*. *J. Gen. Microbiol.* 135:3413–3420.
15. Housden, N. G., S. R. Loftus, ..., C. Kleanthous. 2005. Cell entry mechanism of enzymatic bacterial colicins: porin recruitment and the thermodynamics of receptor binding. *Proc. Natl. Acad. Sci. USA.* 102:13849–13854.
16. Zakharov, S. D., V. Y. Eroukova, ..., W. A. Cramer. 2004. Colicin occlusion of OmpF and TolC channels: outer membrane translocons for colicin import. *Biophys. J.* 87:3901–3911.
17. Yamashita, E., M. V. Zhalnina, ..., W. A. Cramer. 2008. Crystal structures of the OmpF porin: function in a colicin translocon. *EMBO J.* 27:2171–2180.
18. Zakharov, S. D., M. V. Zhalnina, ..., W. A. Cramer. 2006. The colicin E3 outer membrane translocon: immunity protein release allows interaction of the cytotoxic domain with OmpF porin. *Biochemistry.* 45:10199–10207.
19. Sharma, O., K. A. Datsenko, ..., W. A. Cramer. 2009. Genome-wide screens: novel mechanisms in colicin import and cytotoxicity. *Mol. Microbiol.* 73:571–585.
20. Nikaido, H. 2003. Molecular basis of bacterial outer membrane permeability revisited. *Microbiol. Mol. Biol. Rev.* 67:593–656.
21. Oddershede, L., J. K. Dreyer, ..., K. Berg-Sørensen. 2002. The motion of a single molecule, the lambda-receptor, in the bacterial outer membrane. *Biophys. J.* 83:3152–3161.
22. Gibbs, K. A., D. D. Isaac, ..., J. A. Theriot. 2004. Complex spatial distribution and dynamics of an abundant *Escherichia coli* outer membrane protein, LamB. *Mol. Microbiol.* 53:1771–1783.
23. Zakharov, S. D., O. Sharma, ..., W. A. Cramer. 2008. Primary events in the colicin translocon: FRET analysis of colicin unfolding initiated by binding to BtuB and OmpF. *Biochemistry.* 47:12802–12809.
24. Gelles, J., B. J. Schnapp, and M. P. Sheetz. 1988. Tracking kinesin-driven movements with nanometer-scale precision. *Nature.* 331:450–453.
25. Kusumi, A., Y. Sako, and M. Yamamoto. 1993. Confined lateral diffusion of membrane receptors as studied by single particle tracking (nanovid microscopy). Effects of calcium-induced differentiation in cultured epithelial cells. *Biophys. J.* 65:2021–2040.
26. Qian, H., M. P. Sheetz, and E. L. Elson. 1991. Single particle tracking. Analysis of diffusion and flow in two-dimensional systems. *Biophys. J.* 60:910–921.
27. Fujiwara, T., K. Ritchie, ..., A. Kusumi. 2002. Phospholipids undergo hop diffusion in compartmentalized cell membrane. *J. Cell Biol.* 157:1071–1081.
28. Feder, T. J., I. Brust-Mascher, ..., W. W. Webb. 1996. Constrained diffusion or immobile fraction on cell surfaces: a new interpretation. *Biophys. J.* 70:2767–2773.
29. Metropolis, N., A. W. Rosenbluth, ..., E. Teller. 1953. Equation of state calculations by fast computing machines. *J. Chem. Phys.* 21:1087–1092.
30. Ritchie, K., X. Y. Shan, ..., A. Kusumi. 2005. Detection of non-Brownian diffusion in the cell membrane in single molecule tracking. *Biophys. J.* 88:2266–2277.
31. Cadieux, N., C. Bradbeer, and R. J. Kadner. 2000. Sequence changes in the ton box region of BtuB affect its transport activities and interaction with TonB protein. *J. Bacteriol.* 182:5954–5961.
32. Gudmundsdottir, A., P. E. Bell, ..., R. J. Kadner. 1989. Point mutations in a conserved region (TonB box) of *Escherichia coli* outer membrane protein BtuB affect vitamin B12 transport. *J. Bacteriol.* 171:6526–6533.
33. Ritchie, K., and J. Spector. 2007. Single molecule studies of molecular diffusion in cellular membranes: determining membrane structure. *Biopolymers.* 87:95–101.
34. Cadieux, N., P. G. Phan, ..., R. J. Kadner. 2003. Differential substrate-induced signaling through the TonB-dependent transporter BtuB. *Proc. Natl. Acad. Sci. USA.* 100:10688–10693.
35. Steven, A. C., B. Heggeler, ..., J. P. Rosenbusch. 1977. Ultrastructure of a periodic protein layer in the outer membrane of *Escherichia coli*. *J. Cell Biol.* 72:292–301.
36. Leake, M. C., J. H. Chandler, ..., J. P. Armitage. 2006. Stoichiometry and turnover in single, functioning membrane protein complexes. *Nature.* 443:355–358.
37. Zimmer, J., Y. Nam, and T. A. Rapoport. 2008. Structure of a complex of the ATPase SecA and the protein-translocation channel. *Nature.* 455:936–943.
38. Egea, P. F., R. M. Stroud, and P. Walter. 2005. Targeting proteins to membranes: structure of the signal recognition particle. *Curr. Opin. Struct. Biol.* 15:213–220.
39. Driessen, A. J. M., and N. Nouwen. 2008. Protein translocation across the bacterial cytoplasmic membrane. *Annu. Rev. Biochem.* 77:643–667.
40. Jakes, K. S., and A. Finkelstein. 2010. The colicin Ia receptor, Cir, is also the translocator for colicin Ia. *Mol. Microbiol.* 75:567–578.
41. Boon, T. 1972. Inactivation of ribosomes in vitro by colicin E3 and its mechanism of action. *Proc. Natl. Acad. Sci. USA.* 69:549–552.
42. Bowman, C. M., J. E. Dahlberg, ..., M. Nomura. 1971. Specific inactivation of 16S ribosomal RNA induced by colicin E3 in vivo. *Proc. Natl. Acad. Sci. USA.* 68:964–968.
43. Shi, Z., K. F. Chak, and H. S. Yuan. 2005. Identification of an essential cleavage site in ColE7 required for import and killing of cells. *J. Biol. Chem.* 280:24663–24668.
44. Zhang, X. Y. Z., E. L. Goemaere, ..., R. Lloubès. 2009. Mapping the interactions between *Escherichia coli* Tol subunits: rotation of the TolR transmembrane helix. *J. Biol. Chem.* 284:4275–4282.
45. Goemaere, E. L., A. Devert, ..., E. Cascales. 2007. Movements of the TolR C-terminal domain depend on TolQR ionizable key residues and regulate activity of the Tol complex. *J. Biol. Chem.* 282:17749–17757.